

Scaling Behavior of Isotopes in Nuclear Reactions

G. Verde¹, M.B. Tsang¹, C.K. Gelbke¹, T.X. Liu¹, X.D. Liu¹, W.G. Lynch¹, R. Shomin¹, W.P. Tan¹, A. Wagner¹, H.F. Xi¹, H.S. Xu¹, W.A. Friedman², B. Davin³, Y. Laroche³, R.T. de Souza³, R.J. Charity⁴, L.G. Sobotka⁴

¹National Superconducting Cyclotron Laboratory and Department of Physics and Astronomy, Michigan State University, East Lansing, MI 48824, USA

²Department of Physics, University of Wisconsin, Madison, WI 53706

³Department of Chemistry and IUCF, Indiana University, Bloomington, IN 47405, USA

⁴Department of Chemistry, Washington University, St. Louis, MO 63130, USA

Abstract. A three parameter scaling relationship (termed *isoscaling*) between isotopic distributions for elements with $Z \leq 8$ has been observed for a variety of reaction mechanisms that are dominated by phase space, including evaporation, multifragmentation, and deeply inelastic scattering. For multifragmentation processes, the parameters characterizing isoscaling are shown to be sensitive to the density dependence of the asymmetry term of the equation of state. Such sensitivity is discussed within the context of the Expanding Evaporating Source model and an isospin dependent dynamical model of nuclear collisions.

The equation of state (EOS) of strongly interacting matter governs the dynamics of dense matter in supernovae and neutron stars [1]. Experimental investigations with heavy ion collisions, have primarily focused upon terms in the EOS that describe symmetric matter (equal numbers of protons and neutrons), leaving the asymmetry term that reflects the difference between neutron and proton densities largely unexplored [2]. For very asymmetric matter, however, details of this asymmetry term are critically important [1].

Various studies have shown that the mean energy per nucleon $e(\rho, \delta)$ in nuclear matter at density ρ and isospin asymmetry parameter $\delta = (\rho_n - \rho_p) / (\rho_n + \rho_p)$ can be approximated by a parabolic function

$$e(\rho, \delta) = e(\rho, 0) + S(\rho)\delta^2 \quad (1)$$

where $e(\rho, \delta)$ provides the EOS of symmetric matter, and $S(\rho)$ is the symmetry energy [1]. Different functional forms for $S(\rho)$ have been proposed [4], exploring the influence of the density dependence of $S(\rho)$ on nuclear reaction dynamics [3-5].

Calculations of energetic nucleus-nucleus collisions [4,5] reveal that the relative emission of neutrons and protons during the early non-equilibrium stages has a robust sensitivity to the density dependence of $S(\rho)$. In general, pre-equilibrium neutron emission increases relative to pre-equilibrium proton emission for smaller values of the curvature K_{sym} defined as:

$$K_{sym} = 9\rho_0 \left. \frac{\partial^2 S(\rho)}{\partial \rho^2} \right|_{\rho=\rho_0} \quad (2)$$

Enhanced pre-equilibrium neutron emission reduces the neutron-to-proton ratio in the dense region that remains behind [4,5].

In near central Sn+Sn collisions at an incident energy of $E/A=50$ MeV, matter is compressed to densities of about $1.5\rho_0$ before expanding and disassembling into 6-7 fragments with charges of $3 \leq Z \leq 8$ plus assorted light particles. Detailed analyses imply that such multifragment disassemblies occur at an overall density of $\rho \sim \rho_0/6 - \rho_0/3$ and over a time interval of about 30-100 fm/c [6]. Essentially all initial isotopic compositions are determined by the properties of the system during this narrow time frame when the density is significantly less than ρ_0 . This implies that fragment isotopic distributions may have a significant sensitivity to the density dependence of $S(\rho)$.

Unfortunately, the observed isotopic distributions are also influenced by secondary decay, making it very important to identify observables that are insensitive to sequential decay.

Statistical calculations have identified certain ratios of isotopic multiplicities as being robust with respect to the secondary decay [7]. For example, the ratio of the multiplicities $R_{21}(N,Z)=Y_2(N,Z)/Y_1(N,Z)$, of an isotope with neutron number N and proton number Z from two reactions 1 and 2 is relatively insensitive to the distortions from sequential decay. Here we choose the convention that the isospin composition (neutron to proton ratio) of system 2 is larger than that of system 1.

In multifragmentation events, such ratios have been experimentally shown to satisfy a power law relationship [7]:

$$R_{21} = C \cdot \exp(N \cdot \alpha + Z \cdot \beta) \quad (3)$$

The systematics described by Eq. (1) occur naturally within the grand-canonical ensemble [7,8]. In this case the parameters α and β are directly related to the differences between the neutron and proton chemical potentials for the two reactions, $\alpha=\Delta\mu_n/T$ and $\beta=\Delta\mu_p/T$ or the ratios of the free proton and free neutron densities in the two systems, $\hat{\rho}_p = \rho_{p2}/\rho_{p1}$ and $\hat{\rho}_n = \rho_{n2}/\rho_{n1}$. C is an overall normalization constant.

The accuracy of the scaling behavior described by Eq. (1) can be compactly displayed if one plots the scaled isotopic ratio,

$$S(\beta) = R_{21} \cdot \exp(-\beta Z) \quad (4)$$

as a function of N . For all elements, $S(N)$ must lie along a straight line on a semi-log plot when Eq. (2) accurately describes the experimental data. The data points marked as "multifragmentation" in Figure 1 show values of $S(N)$ extracted from isotope yields with $1 \leq Z \leq 8$ measured for multifragmentation events in central $^{124}\text{Sn}+^{124}\text{Sn}$ and $^{112}\text{Sn}+^{112}\text{Sn}$ collisions at $E/A=50$ MeV [7].

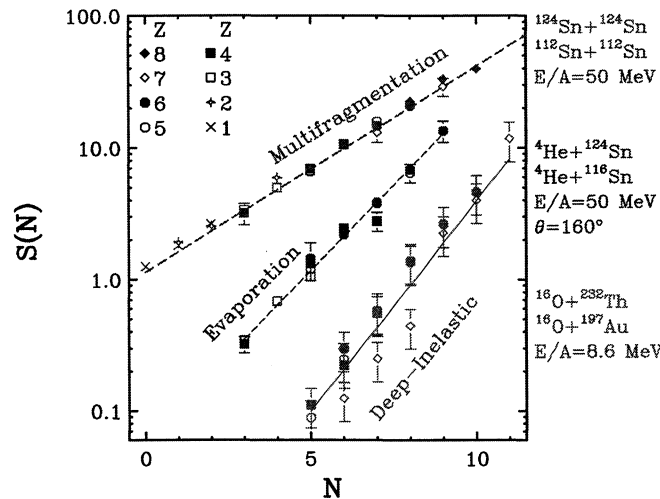


FIGURE 1. Isoscaling behavior observed in different nuclear reactions.

The extracted values of α and β are 0.36 and -0.4 respectively. This scaling behavior, referred as *iso-scaling* [9], appears to be a surprisingly robust feature of the data under a wide range of circumstances [9].

First we consider deep-inelastic ^{16}O induced reactions on two targets ^{232}Th and ^{197}Au [10]. Iso-scaling behavior, with $\alpha=0.74$ and $\beta=-1.1$, is observed, as shown in Fig. 1 close the label "deep-inelastic". In damped binary collisions at low incident energies ($E/A < 10\text{MeV}$), equilibrium is well established between the orbiting projectile and target. In such cases, the isotopic yields follow the "Q_{gg}-systematics"[10,11], and can be approximated by

$$Y(N,Z) \propto \exp[(M_p + M_T - M'_p - M'_T)/T] \quad (5)$$

where M_P and M_T are the initial projectile and target masses, and M'_p and M'_t are the final masses. Expanding the nuclear binding energy contributions to the masses in Taylor series in N and Z and truncating the expansion to the first order in N and Z , we obtain an approximated expression for the isotope ratio defined in Eq. (1):

$$R_{21} \propto \exp\left[\frac{-\Delta s_n \cdot N - \Delta s_p \cdot Z}{T}\right] \quad (6)$$

where Δs_n and Δs_p are the differences of the neutron and proton separation energies for the two compound systems.

Eq. (4) explains why isoscaling is observed in deep-inelastic collisions, where the difference in the average separation energies in Eq. (4) plays a corresponding role to the difference in chemical potentials in the grand canonical approach.

Next we consider the yields from processes involving the formation of a composite system and its subsequent decay via the evaporation of different isotopes. Corresponding scaled isotopic ratios for fragments detected at backward laboratory angles ($\theta = 160^\circ$) in ${}^4\text{He}+{}^{116}\text{Sn}$ and ${}^4\text{He}+{}^{124}\text{Sn}$ collisions at $E/A=50$ MeV [12] are shown in Fig. 1, next to the label “evaporation”. Within the context of the formalism proposed by Friedman and Lynch [13], based on the detailed balance principle, the ratio between the evaporation yields of the isotope (N, Z) in reactions 2 and 1 can be expressed as

$$R_{21}(N, Z) \propto \exp\left\{\left[(-\Delta s_n + \Delta f_n^*) \cdot N + (-\Delta s_p + \Delta f_p^* + e\Delta\Phi(Z_i - Z)) \cdot Z\right] / T\right\} \quad (7)$$

$\Phi(Z)$ is the electrostatic potential at the surface of a nucleus with proton number Z and Z_i is the proton number of the parent nucleus. Δs_n (Δs_p) is the difference of the neutron (proton) separation energy for the two compound systems. Δf_n^* (Δf_p^*) is the difference between the excitation contributions to the free energy per neutron (proton). Aside from the second order term from the electrostatic potential, which is small for the decay of large nuclei, all factors in the exponent are proportional to either N or Z , consistent with Eq. (1). The corresponding scaling parameters α and β , are functions of the separation energies, the Coulomb potential and small contributions from the free excitation energies. The experimental values obtained for these parameters are $\alpha=0.6$ and $\beta=-0.82$. The explored systematics of nuclear reactions suggests that iso-scaling is obeyed where 1.) both reactions 1 and 2 are accurately described by a specific statistical fragment emission mechanism and 2.) both systems are at nearly the same temperature [9]. In the next section we will show that the α and β parameters extracted from multifragmentation data, are sensitive to the density dependence of asymmetry energy in the nuclear EOS, as it will be shown in the next section.

ACCESSING THE ASYMMETRY TERM IN THE NUCLEAR EOS

Predictions of the Expanding Evaporating Source Model

The Expanding Evaporating Source (EES) model [13,14] describes multifragmentation as an evaporation of fragments from the surface of an expanding system. Calculating the isotope ratio R_{21} , defined in Eq. (1), it is possible to show [9] that the asymmetry term, $Sym(\rho) \cdot (N-Z)^2 / A$, provides the dominant contribution to the coefficient α . For simplicity, we assumed a power law density dependence $Sym(\rho) = C_{sym} \cdot (\rho / \rho_0)^\gamma$, where γ is a variable and $C_{sym}=23.4$ MeV is the conventional liquid drop model constant [9].

We have performed calculations for the decay of the composite systems found in ${}^{124}\text{Sn}+{}^{124}\text{Sn}$ and ${}^{112}\text{Sn}+{}^{112}\text{Sn}$ collisions assuming, for simplicity, initial systems of $(Z_{\text{tot}}, A_{\text{tot}})$ of (100, 248) and (100, 224), respectively, initial thermal excitation energies of $E_{\text{ther}}^*=9.5$ MeV, and initial collective radial expansion energies of $E_{\text{Coll}}/A=2.5$ MeV. The fragments are emitted from these systems as they expand from an initial density $\rho/\rho_0=1$ to $\rho/\rho_0=0.1$. The left panel of Figure 2 shows two iso-scaling functions, $S(N)$, calculated with the predicted isotope yields for $3 \leq Z \leq 6$ for $\gamma=1$ and $\gamma=0$. Values for α , shown in the right panel as a function of γ , are determined from the slopes of best fit of the lines to the predicted iso-scaling functions.

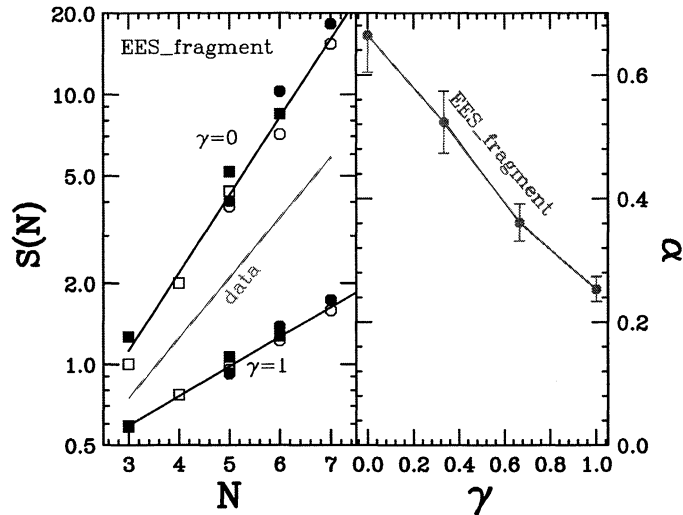


FIGURE 2. EES model predictions for the scaling function $S(N)$ (left panel) and the scaling parameter α (right panel). See text.

The EES model predicts that α is sensitive to the value of γ , describing the stiffness of the density dependence of the symmetry energy. The multifragmentation data in Fig. 1 can be fairly well reproduced by $\gamma \sim 0.6$.

Predictions of Isospin Dependent Transport Theories

The sensitivity of the iso-scaling parameters α and β to the symmetry term of the nuclear EoS has been investigated also in the context of an isospin dependent transport theory [4,16].

The solid circles and squares in Fig. 3 show values for α and β , respectively, obtained from fragments with $3 \leq Z \leq 8$ detected in central $^{112}\text{Sn}+^{112}\text{Sn}$, $^{112}\text{Sn}+^{124}\text{Sn}$ and $^{124}\text{Sn}+^{124}\text{Sn}$ collisions at $E/A=50$ MeV [7]. The $^{112}\text{Sn}+^{112}\text{Sn}$ reaction was labeled as 1 in Eq. 2; the different data points correspond to the three choices for reaction 2 and are plotted in both left and right panels as a function of $N_{\text{tot}}/Z_{\text{tot}}$ where N_{tot} and Z_{tot} are the total numbers of neutrons and protons involved in reaction 2.

As discussed previously, the isospin asymmetries of the excited systems prior to multifragment breakup are sensitive to the density dependence of the asymmetry term of the EOS [4,5]. The "prefragment" is reduced in size relative to the total system by preequilibrium emission when it disintegrates into the final fragments. Different calculations based on transport theories predict preequilibrium emission that is increasingly neutron-deficient and corresponding prefragments that are more neutron-rich for larger values of K_{sym} [4,5].

We examined the isotopic effects shown in Fig. 3 using a hybrid model. Specifically, we solved the BUU equation [16] to obtain predictions for the dynamical emission of light particles during the compression and expansion stages of the collision. In this first step, the mean field for symmetric nuclear matter in the BUU calculations was chosen to have a stiff EOS ($K = 386$ MeV). Calculations were performed with two different expressions for the asymmetry term, "asy-stiff" ($K_{\text{sym}}=61$ MeV) and "asy-soft" ($K_{\text{sym}}= -69$ MeV) [4,5]. After an elapsed time of 100 fm/c, the central density decreased to a value of about $\rho_0/6$. The regions with densities $\rho/\rho_0 > 1/8$ were then isolated and their decay was calculated with the Statistical Multifragmentation Model (SMM) of ref. [15]. Secondary decays of excited primary fragments are calculated by carefully accounting for their internal level structure and branching ratios [15]. The isotopic ratios in Fig. 1 were then calculated from the final isotopic distributions. The open rectangles indicate the ratios obtained from the yields of primary fragments and the cross-hatched rectangles indicate the ratios obtained from the yields of the final fragments after secondary decay. The vertical height of each rectangle reflects the range of values for each quantity as the assumed excitation energy is varied over the range of $E^*/A = 4-6$ MeV.

The left and right panels in Fig. 3 provide values calculated for prefragments obtained with the asy-stiff and asy-soft EOS's, respectively. In both panels, it can be seen that the ratios calculated from the primary yields (open rectangles) and those calculated from the secondary yields (cross-hatched rectangles) are similar, indicating that values for $R_{2j}(N,Z)$ are relatively insensitive to secondary decays. The ratios corresponding to the asy-stiff EOS (left

panel) overlap the data and show a significantly stronger dependence on N_{tot}/Z_{tot} , than do the results of the asy-soft EOS (right panel).

The results of the hybrid model approach confirm a sensitivity of the isotopic fragment yields to the asymmetry term of the EOS. However, the details of this sensitivity are model dependent. The hybrid model predicts that an asy-stiff EOS leads to fragments that are more neutron-rich than those produced when the EOS is asy-soft. This trend is opposite to the one predicted by the Expanding Evaporative Source (EES) model (see left panel in Fig. 2), which assumes the fragments originate from surface emission and not from the equilibrium decay of the residue.

In summary, we have shown the existence of a scaling behavior of isotopes emitted in nuclear collisions governed by different reaction mechanisms. The parameters characterizing such isoscaling phenomena, in multifragmentation decay of excited nuclear systems, display a significant sensitivity to the density dependence of the asymmetry term in the nuclear EoS. However, the observed model dependency of the details of such sensitivity suggest that it would be desirable to explore further the connection between the fragment isotopic distributions and the EoS both experimentally and within the context of other dynamical and statistical models.

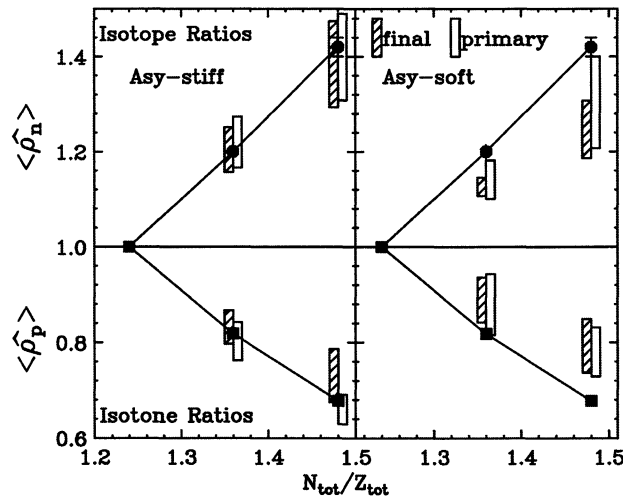


FIGURE 3. The solid circles and squares show values for $\hat{\rho}_n$ and $\hat{\rho}_p$, respectively, measured in central $^{112}\text{Sn}+^{112}\text{Sn}$ and $^{124}\text{Sn}+^{124}\text{Sn}$ collisions at $E/A=50$ MeV. The open and cross-hatched rectangles show hybrid calculation results from the primary and final fragment yields, respectively, using an Asy-stiff (left panel) and an Asy-soft (right panel) EoS. See text.

REFERENCES

1. J.M. Lattimer and M. Prakash, Ap. J. 550, 426 (2001); J.M. Lattimer and M. Prakash, Phys. Rep. 333, 121 (2000)
2. D.H. Youngblood et al., Phys. Rev. Lett. 82, 691 (1999); H.L. Clark et al., Phys. Rev. C 63, 031301(R) (2001)
3. M. Prakash et al., Phys. Rev. Lett. 61, 2518 (1998)
4. Bao-An Li, Phys. Rev. Lett. 85, 4221 (2000), Bao-An Li et al., Phys. Rev. Lett. 78, 1644 (1997)
5. V. Baran et al., Nucl. Phys. A632, 287 (1998), L. Scalone et al., Phys. Lett. B461, 9 (1999)
6. B. Borderie et al., Phys. Rev. Lett. 86, 3252 (2001), T. Glasmacher et al., Phys. Rev. C50, 952 (1994), L. Beaulieu et al., Phys. Rev. Lett. 84, 5971 (2000).
7. H. S. Xu et al., Phys. Rev. Lett. 85, 716 (2000). M.B Tsang et al., Phys. Rev. C 64, 054615 (2001)
8. J. Randrup and S.E. Koonin, Nucl. Phys. A356, 223 (1981), S. Albergo et al., Il Nuovo Cimento 89A, 1 (1985)
9. M.B. Tsang et al., Phys. Rev. Lett. 86, 5023 (2001), M.B. Tsang et al., Phys. Rev. C 64, 041603(R) (2001)
10. V.V. Volkov, Phys. Rep. 44, 93, (1978)
11. C.K. Gelbke et. al., Phys. Rep. 42, 311 (1978)
12. J. Brzychczyk et al., Phys. Rev. C47, 1553 (1993)
13. W. Friedman and W. Lynch, Phys. Rev. C 28, 950 (1983)
14. W.A. Friedman, Phys. Rev. Lett, 2125 (1988), W.A. Friedmann, Phys. Rev. C42, 667 (1990)
15. S.R. Souza, W.P. Tan, R. Donangelo, C.K. Gelbke, W.G. Lynch, M.B. Tsang, Phys. Rev. C62, 064607 (2000)
16. W. Tan et al., Phys. Rev. C 64, 051901 (2001)